

## Thermodynamic properties of the nonzero-temperature, quantum-mechanical, one-component plasma\*

M. A. Pokrant†

*Department of Physics and Astronomy, University of Florida, Gainesville, Florida 32611*

(Received 16 June 1976)

The thermodynamic properties of the quantum-mechanical one-component plasma are calculated at all temperatures for four densities at the high-density end of the metallic region. The Slater sum (diagonal density matrix) is obtained by using a nonzero-temperature variational principle with the simplest credible approximations. The Slater sum is approximated as the product of the ideal Fermi-gas Slater sum and a product of pair functions. Various methods for calculating thermodynamic quantities are investigated with the main emphasis on the pressure. In calculating the thermodynamic properties, the effects of Fermi statistics are included in a nonperturbative manner using Lado's method. The hypernetted-chain approximation is used to compute the pair correlation functions. Three different approximations are used for the three-body correlation functions so that errors may be estimated. The free energy is calculated by integrating the energy over temperature, while holding the volume fixed. Differentiating the free energy with respect to volume was found to yield more accurate pressures than using the virial theorem. Tables of the excess energies, pressures, and free energy are given for four densities and 20 temperatures.

### I. INTRODUCTION

The object of this paper is to calculate the thermodynamic properties of the quantum-mechanical one-component plasma (OCP) at all temperatures. The OCP consists of  $N$  Coulomb charges in a box of volume  $\Omega$  with a uniform neutralizing background. The contribution of the background to the thermodynamic quantities must always be subtracted out. This system is equivalent to the ground-state quantum electron gas for very low temperatures and to the classical one-component plasma at very high temperatures.

A previous paper,<sup>1</sup> relevant parts of which are outlined in Sec. II, showed how to obtain the Slater sum (diagonal density matrix) at all temperatures by using a non-zero-temperature variational principle (NZTVP) for the Slater sum,<sup>2,3</sup> together with the simplest credible approximations. The results of that paper are extended to four densities,  $r_s = 0.5, 1.0, 2.0, 3.39$ , where  $r_s$  is the ion-sphere radius in Bohr radii

$$r_s = (3/4\pi\rho)^{1/3}/a_0. \quad (1.1)$$

Various methods for calculating thermodynamic quantities are investigated here, with the main emphasis on the pressure. The third section gives the methods used to compute the energies. The effects of Fermi statistics are included in a simple, nonperturbative manner by using Lado's method.<sup>4,5</sup> The hypernetted-chain (HNC) approximation<sup>6</sup> is used to compute the pair correlation functions. Three different approximations for the three-body correlation functions are used so that errors may be estimated. The best method for obtaining the pressure was found to be differentia-

ting the free energy with respect to volume. The free energy is calculated by integrating the energy over temperature, while holding the volume fixed. Once the free energy has been calculated, other thermodynamic quantities may be obtained. Section IV gives the numerical methods used and summarizes the results. Section V discusses these results and indicates how the approximations could be improved. Alternative methods for obtaining thermodynamic quantities are given in the Appendix. While these methods gave poor results for the OCP, they may be useful for other systems. Also, they allow us to estimate the size of a term which was neglected.

### II. OBTAINING THE SLATER SUM

The quantity of interest at nonzero temperatures is the Slater sum (diagonal density matrix), defined as

$$W = N! \lambda^{3N} \sum_n (e^{-\beta H/2} \Psi_n)^* (e^{-\beta H/2} \Psi_n), \quad (2.1)$$

where  $\beta = 1/kT$ ,  $\lambda^2 = 2\pi\hbar^2\beta/m$ , the sum is over any complete set of wave functions with the proper symmetry, and  $H$  is the Hamiltonian operator. We write the Slater sum as

$$W = e^{-U_t}, \quad (2.2)$$

where  $U_t$ , the total quantum potential, is defined by Eq. (2.2). By differentiating Eq. (2.1) with respect to  $\beta$ , we obtain a differential equation for  $U_t$

$$\begin{aligned} F_t[U_t] = & -\frac{\partial U_t}{\partial \beta} + V_{c1} \\ & + \frac{\hbar^2}{4m} \sum_i (\nabla_i^2 U_t - \frac{1}{2} \nabla_i U_t \cdot \nabla_i U_t) + Y \\ = & 0, \end{aligned} \quad (2.3)$$

where  $V_{cl}$  is the classical interaction potential and  $Y$  is defined in Refs. 1 and 2;

$$Y = -\frac{\hbar^2}{8m} \sum_i \nabla_i U_i \cdot \nabla_i U_i - \frac{3N}{2\beta} + \frac{\hbar^2 N! \lambda^{3N}}{2mW} \sum_i \sum_n \nabla_i (e^{-\beta H/2} \Psi_n)^* \cdot \nabla_i (e^{-\beta H/2} \Psi_n).$$

The term  $Y$  contains the effects of antisymmetry and for low temperatures these effects will not be negligible. For this reason we differentiate the Slater sum for an ideal noninteracting gas of fermions with respect to  $\beta$  and subtract the corresponding result from Eq. (2.3) to obtain

$$F[U] = -\frac{\partial U}{\partial \beta} + V_{cl} + \frac{\hbar^2}{4m} \sum_i \left( \nabla_i^2 U - \frac{1}{2} \nabla_i U \cdot \nabla_i U + \frac{\nabla_i U \cdot \nabla_i W_i}{W_i} \right) + Y - Y_I = 0, \quad (2.4)$$

where  $U$ , the quantum potential, is defined by

$$W = W_I e^{-U}. \quad (2.5)$$

We feel safe in neglecting  $Y - Y_I$  because the effects of antisymmetry are presumably<sup>7,8</sup> the same in both  $Y$  and  $Y_I$  (approximation 1). The boundary condition is

$$U \rightarrow \beta V_{cl} \text{ as } \beta \rightarrow 0. \quad (2.6)$$

The NZTVP consists of minimizing the functional<sup>2</sup>

$$J[U] = \left( \int W_I e^{-U} dR \right)^{-1} \int W_I e^{-U} F[U] dR \quad (2.7)$$

with respect to arbitrary variations of  $U$  while holding  $\partial U/\partial \beta$  fixed. The integrations are over all particle positions. It can be shown<sup>2</sup> that, if we use the exact  $\partial U/\partial \beta$ , then  $J[U]$  has a single minimum of zero for the exact  $U$ , except that  $U$  is only

determined to within an additive function,  $f(N, \Omega, T)$ , which does not depend on the particle positions.

An integration by parts allows us to write  $J$  as

$$J[U] = \left( \int W_I e^{-U} dR \right)^{-1} \times \int W_I e^{-U} \left( -\frac{\partial U}{\partial \beta} + V_{cl} + \frac{\hbar^2}{8m} \sum_i \nabla_i U \cdot \nabla_i U \right) dR. \quad (2.8)$$

We then approximate  $U$  as a sum of pair functions (approximation 2),

$$U = \sum_{i < j} u(r_{ij}), \quad (2.9)$$

and use the Bohm-Pines random-phase approximation<sup>9</sup> (RPA) as used by Dunn and Broyles<sup>10,11</sup> to approximate the three-body terms which come from  $\nabla U \cdot \nabla U$  (approximation 3). This gives

$$J[\tilde{u}] \cong \frac{1}{2} N \rho \int \left[ \tilde{G}(k) \left( \frac{4\pi e^2}{k^2} - \frac{\partial \tilde{u}}{\partial \beta} \right) + \frac{\hbar^2 k^2}{4m} (1 + \rho \tilde{G}) \tilde{u}^2 \right] \frac{d\tilde{k}}{(2\pi)^3}, \quad (2.10)$$

where  $\rho$  is the density, the tilde denotes the Fourier transform, defined by

$$\tilde{G}(k) = \int e^{i\mathbf{k} \cdot \mathbf{r}} G(r) d\mathbf{r}, \quad (2.11)$$

and  $G(r)$  is the radial distribution function minus 1,  $G = g - 1$ .

The NZTVP strictly holds only if  $\partial u/\partial \beta$  is exact. In practice we try to achieve self-consistency between  $\partial u/\partial \beta$  and the  $u$  determined by minimizing  $J$  at each temperature.

Defining  $\gamma = \epsilon_p/\epsilon_F$ , where  $\epsilon_p$  is the plasma energy defined as  $\epsilon_p = \hbar \omega_p = (4\pi \rho e^2 \hbar^2/m)^{1/2}$  and  $\epsilon_F$  is the Fermi energy defined as  $\epsilon_F = \hbar^2 k_F^2/2m$ ,  $k_F = (3\pi^2 \rho)^{1/3}$ , and using Fermi units so that  $k_F = 1$ , Eq. (2.8) may be put into the form<sup>1</sup>

$$J[\tilde{u}, \partial \tilde{u}/\partial \beta] = N \epsilon_F \left( \frac{3\gamma^2}{8} \int_0^\infty (S-1) dk - \frac{1}{4\pi^2} \int_0^\infty (S-1) \frac{\partial \tilde{u}}{\epsilon_F \partial \beta} k^2 dk + \frac{1}{24\pi^4} \int_0^\infty S \tilde{u}^2 k^4 dk \right), \quad (2.12)$$

where  $S = 1 + \rho \tilde{G}$  is the structure factor.

The fourth approximation is to use the Gaskell-Broyles-Sahlin-Carley (GBSC) structure factor,<sup>12</sup> essentially an obvious generalization of the RPA,

$$S(k) \cong S_I(k) / (1 + \rho \tilde{u}(k) S_I(k)), \quad (2.13)$$

where  $S_I$  is the structure factor for an ideal Fermi gas which is calculated from the equation in Lado's paper.<sup>4</sup> This fourth approximation has the advantage of not requiring an iterative calculation.

It also eliminates the necessity of computing the ideal-gas effective potentials since only  $S_I$  and not  $U_I$  is needed to compute  $S$ . This is because Eq. (2.13) is a perturbation formula for  $S$ . In the limit of vanishing  $u$ ,  $S$  reduces to  $S_I$ . Thus, we expect this approximation to be very good at high densities where the system most nearly resembles an ideal gas. The approximations have simplified the problem of computing  $J$  for a given  $u$  and  $\partial u/\partial \beta$  to a single one-dimensional integral with no

iterating necessary.

The quantum pair potential  $u(r)$  was chosen to be of the form suggested by Dunn and Broyles<sup>10</sup> and used by Stevens<sup>13</sup> and others<sup>14,15</sup> in the ground state (approximation 5). It is given by

$$u(r) = (a/4\pi\tau'r)(1 - e^{-r(b\tau')^{1/2}}), \quad (2.14)$$

where  $b$  is the variational parameter,

$$\tau' = \frac{1}{2}\gamma \coth \frac{1}{2}\beta \epsilon_p, \quad (2.15)$$

and

$$a = \frac{3}{2}\pi^2\gamma^2. \quad (2.16)$$

The quantity  $a$  was determined by solving the Euler-Lagrange equation (i.e.,  $\delta J/\delta \tilde{u} = 0$ ) at small  $k$  as was done in Ref. 16.

With  $\tilde{u}$  depending on  $b$  and with  $b$  replaced by  $c$  in  $\partial \tilde{u}/\partial \beta$  so that  $\partial \tilde{u}/\partial \beta$  is a trial function which depends on  $c$  and  $\partial c/\partial \beta$ , we have a self-consistent solution if

$$\left[ \frac{\partial J[\tilde{u}(b), \partial \tilde{u}(c)/\partial \beta]}{\partial b} \right]_{b=c} = 0 \quad (2.17)$$

at all temperatures, i.e., when the trial function and the  $\tilde{u}(b)$  determined by minimization are in agreement.

Using Eqs. (2.12), (2.13), and (2.14), we can then solve Eq. (2.17) for  $\partial c/\partial \beta$  to obtain

$$\begin{aligned} \frac{1}{\epsilon_F} \frac{\partial c}{\partial \beta} = & \left( \int_0^\infty \frac{k^2 S^2}{q^4} dk \right)^{-1} \\ & \times \int_0^\infty \frac{k^2 S^2}{q^4} [qc(1 - S_T^{-1}) + k^2(1 - c) \\ & + c(2 - c)\tau'] dk, \quad (2.18) \end{aligned}$$

where  $q = k^2 + c\tau'$ . The improved Euler method<sup>17</sup> with a variable step size was used to numerically integrate this equation down from  $T = \infty$ . It is easy to show that in the limit of very high temperatures

$$c \rightarrow \frac{3}{2} \text{ as } T \rightarrow \infty. \quad (2.19)$$

The integration was actually started from  $\beta\epsilon_F = 0.02$ . Table I contains a list of the  $c$ 's determined as a function of  $\tau$  and  $r_s$ , where  $\tau$  is the temperature in Fermi units,

$$\tau = kT/\epsilon_F. \quad (2.20)$$

Approximation 2 of this section, the pair approximation for  $U$ , is reasonable because the infinite-temperature limit of  $U$  is a sum of pair functions and the ground-state energy results of Ref. 13 and their agreement with the high-density series show that the pair approximation is quite good. Reference 13 also tested the form chosen for  $u$  (approximation 5). It showed that this form

TABLE I. Values of the parameter  $c$  as a function of  $\tau = kT/\epsilon_F$  and  $r_s$ , the ion-sphere radius. The infinite temperature limit is 1.500.

$\tau \backslash r_s$	0.50	1.00	2.00	3.39
0	0.795	0.918	1.030	1.104
0.05	0.800	0.922	1.032	1.105
0.10	0.816	0.931	1.037	1.108
0.20	0.899	0.973	1.056	1.118
0.50	1.157	1.155	1.163	1.176
0.80	1.284	1.268	1.254	1.244
1.00	1.332	1.316	1.297	1.282
1.33	1.382	1.367	1.347	1.329
1.60	1.407	1.393	1.375	1.358
2.00	1.431	1.419	1.403	1.387
2.29	1.443	1.432	1.418	1.403
2.67	1.454	1.445	1.432	1.419
3.20	1.465	1.458	1.447	1.436
4.00	1.475	1.470	1.461	1.452
5.33	1.484	1.480	1.475	1.468
8.00	1.491	1.489	1.486	1.481
10.00	1.494	1.492	1.490	1.488
12.50	1.495	1.495	1.493	1.491
16.67	1.497	1.497	1.496	1.495
20.00	1.498	1.498	1.497	1.496
25.00	1.499	1.498	1.498	1.497

was excellent for  $r_s \geq 1.0$ , but caused an error of about 3% in the correlation energy at  $r_s = 0.5$ . Both approximations 3 and 4 are expected to be good for high densities and poor for low densities, but improving as the temperature increases. The lowest density studied here,  $r_s = 3.39$ , is probably the absolute extreme for which these approximations should be used at  $T = 0$ .

### III. METHODS FOR OBTAINING THERMODYNAMIC QUANTITIES

Once we have obtained the parameter  $b$ , and hence  $U$ , as a function of temperature and density, we can use more accurate approximations to obtain the energy than were used to get  $b$ . We do this because we expect energies calculated from an approximate Slater sum to be more accurate than the Slater sum from which it is calculated, just as an energy calculated from an approximate ground-state wave function is more accurate than the wave function from which it is calculated. In calculating the energy from the Slater sum we propose to improve approximations 3 and 4 made in calculating the Slater sum in Sec. II. The random-phase approximation<sup>9</sup> as used by Dunn and Broyles<sup>10</sup> (approximation 3) will be replaced separately by both the Kirkwood superposition approximation<sup>18</sup> (KSA) and the convolution approximation<sup>19</sup> (CA) in the energy calculation.

The GBSC structure factor<sup>12</sup> (approximation 4) used in Sec. II will be replaced by the more accurate HNC approximation<sup>6</sup> in determining the energy. The HNC approximation was chosen because it has been shown to be very accurate for the classical Coulomb plasma.<sup>20</sup> This will necessitate expressing  $W_I$  in terms of  $u_I$ , the ideal-Fermi-gas pair potential, which was unnecessary as long as the GBSC perturbation formula was used for the structure factor.

$$W_I = e^{-U_I} = \exp\left(-\sum_{i < j} u_I(r_{ij})\right). \quad (3.1)$$

To be consistent we will invert the HNC integral equation to obtain  $u_I$  from  $g_I$ , rather than using Lado's method<sup>4,5</sup> to obtain  $u_I$ .

We obtain the energy by differentiating the parti-

$$E = \frac{3N}{2\beta} + \frac{1}{Z} \int e^{-U_I} \left( \frac{\partial U_I}{\partial \beta} + V_{c1} + \frac{\hbar^2}{4m} \sum_I (\nabla_I^2 U - \frac{1}{2} \nabla_I U \cdot \nabla_I U - \nabla_I U \cdot \nabla_I U_I) \right) dR. \quad (3.6)$$

Integrating by parts and subtracting the corresponding expression for the ideal-gas energy gives the excess energy

$$E - E_I = \int \left( \frac{e^{-U_I}}{Z} - \frac{e^{-U_I}}{Z_I} \right) \frac{\partial U_I}{\partial \beta} dR + \frac{1}{Z} \int e^{-U_I} \left( V_{c1} + \frac{\hbar^2}{8m} \sum_I \nabla_I U \cdot \nabla_I U \right) dR. \quad (3.7)$$

In terms of the pair functions,  $u$  and  $u_I$ , the excess energy per particle,

$$\epsilon = (E - E_I)/N \quad (3.8)$$

may be written as

$$\epsilon = P + K, \quad (3.9)$$

where  $P$  is the potential energy per particle of the system,

$$P = \frac{1}{2} \rho \int G \frac{e^2}{r} d\vec{r} \quad (3.10)$$

and

$$K = K_1 + K_2, \quad (3.11)$$

is the excess kinetic energy per particle of the system.

$$K_1 = \frac{1}{2} \rho \int (g - g_I) \frac{\partial u_I}{\partial \beta} d\vec{r}, \quad (3.12)$$

$$K_2 = \frac{\hbar^2}{8m} \rho \int g \nabla u \cdot \nabla u d\vec{r} + \frac{\hbar^2}{8m} \rho^2 \int \nabla_1 u(r_{12}) \cdot \nabla_1 u(r_{13}) \times g^{(3)}(r_{12}, r_{13}, r_{23}) d\vec{r}_{12} d\vec{r}_{13}. \quad (3.13)$$

tion function,

$$Q_N(\Omega, T) = (\lambda^{3N} N!)^{-1} \int W dR, \quad (3.2)$$

with respect to  $\beta$ . Thus,

$$E = - \left( \frac{\partial \ln Q_N(\Omega, T)}{\partial \beta} \right)_{\Omega, N} = \frac{3N}{2\beta} + \frac{1}{Z} \int W \frac{\partial (U + U_I)}{\partial \beta} dR, \quad (3.3)$$

$$Z = \int W dR, \quad (3.4)$$

$$U_t = U + U_I. \quad (3.5)$$

Since  $\partial U/\partial \beta$  is not completely determined (see Sec. II) because of the additive function  $\partial f(N, \Omega, T)/\partial \beta$ , we must put Eq. (3.3) into a form in which  $f$  does not appear. We use Eq. (2.4) for  $\partial U/\partial \beta$  in Eq. (3.3) to obtain

$K_2$  is the part of the energy approximated by the RPA in arriving at the Slater sum in Sec. II.

It is usually best to calculate  $P$  and  $K_1$  in Fourier transform space owing to the fact that the integrals in  $k$  space are less sensitive to changes in range and increment. They are

$$P = \frac{1}{2} \int [S(k) - 1] \frac{4\pi e^2}{k^2} \frac{d\vec{k}}{(2\pi)^3} \quad (3.14)$$

and

$$K_1 = \frac{1}{2} \int [S(k) - S_I(k)] \frac{\partial \tilde{u}_I}{\partial \beta} \frac{d\vec{k}}{(2\pi)^3}. \quad (3.15)$$

It is easy to show that the RPA as used by Dunn and Broyles, approximation 3 of Sec. II, gives

$$K_2^{\text{RPA}} = \frac{\hbar^2}{8m} \rho \int k^2 \tilde{u}^2 S(k) \frac{d\vec{k}}{(2\pi)^3}. \quad (3.16)$$

Stevens<sup>13</sup> gives the expression for  $K_2$  if we use the CA for  $g^{(3)}$ ,

$$g_{CA}^{(3)} = g(r_{12})g(r_{13})g(r_{23}) - G(r_{12})G(r_{13})G(r_{23}) + \rho \int G(r_{14})G(r_{24})G(r_{34}) d\vec{r}_4. \quad (3.17)$$

The result is

$$K_2^{\text{CA}} = K_2^{\text{RPA}} + \frac{\hbar^2}{8m} \rho \int G(r) \left( \frac{dQ(r)}{dr} \right)^2 d\vec{r}, \quad (3.18)$$

where

$$\tilde{Q}(k) = \tilde{u}(k)S(k). \quad (3.19)$$

If we use the KSA for  $g^{(3)}$ ,

$$g_{KSA}^{(3)} = g(r_{12})g(r_{13})g(r_{23}), \quad (3.20)$$

we obtain

$$K_2^{\text{KSA}} = K_2^{\text{RPA}} + \frac{\hbar^2}{8m} \rho \left[ \int G(r) \left( \frac{du}{dr} \right)^2 d\vec{r} + \rho \int \left( 2k\bar{u} + \frac{d\bar{L}}{dk} \right) \frac{d\bar{L}}{dk} \bar{G}(k) d\vec{k} \right], \quad (3.21)$$

where

$$L(r) = \frac{G(r)}{r} \frac{du}{dr}. \quad (3.22)$$

The integrations were carried out by the same procedure as in Ref. 13. The potential energy and excess kinetic energies for each of the three approximations are listed for four densities as a function of  $\tau$ , in Tables II–V. In Ref. 13, the CA to the energy was minimized. Here we used the methods of Sec. II to obtain the Slater sum and then calculated the energy using the CA. Figure 1 compares our results for the correlation energy ( $\epsilon$  minus exchange energy) using the CA for  $T=0$  with the results of Ref. 13 and with the high-<sup>21</sup> and low-density<sup>22</sup> expansions for the correlation energy.

The most direct way to obtain the excess pressure, total pressure minus ideal Fermi gas pressure

TABLE II. Computed values of potential energy  $P$  and excess kinetic energy  $K$  per particle as a function of  $\tau = kT/\epsilon_F$  for  $r_s = 0.50$ . The excess kinetic energy is given for the convolution approximation (CA), the Kirkwood superposition approximation (KSA), and the random-phase approximation (RPA). All energies are in rydbergs.

$\tau$	$-P$	$K^{\text{CA}}$	$K^{\text{KSA}}$	$K^{\text{RPA}}$
0	2.098	0.125	0.131	0.142
0.05	2.094	0.126	0.131	0.143
0.10	2.085	0.124	0.129	0.141
0.20	2.054	0.103	0.108	0.123
0.50	1.894	-0.020	-0.018	0.004
0.80	1.725	-0.095	-0.094	-0.074
1.00	1.627	-0.119	-0.119	-0.100
1.33	1.490	-0.136	-0.136	-0.121
1.60	1.399	-0.139	-0.139	-0.127
2.00	1.287	-0.137	-0.137	-0.127
2.29	1.220	-0.132	-0.132	-0.124
2.67	1.145	-0.125	-0.125	-0.119
3.20	1.058	-0.116	-0.116	-0.111
4.00	0.957	-0.103	-0.103	-0.099
5.33	0.837	-0.086	-0.086	-0.084
8.00	0.687	-0.064	-0.064	-0.063
10.00	0.615	-0.054	-0.054	-0.053
12.50	0.549	-0.045	-0.045	-0.044
16.67	0.474	-0.035	-0.035	-0.035
20.00	0.431	-0.030	-0.030	-0.030
25.00	0.384	-0.024	-0.024	-0.024

TABLE III. Computed values of potential energy  $P$  and excess kinetic energy  $K$  per particle as a function of  $\tau = kT/\epsilon_F$  for  $r_s = 1.00$ . The excess kinetic energy is given for the convolution approximation (CA), the Kirkwood superposition approximation (KSA) and the random-phase approximation (RPA). All energies are in rydbergs.

$\tau$	$-P$	$K^{\text{CA}}$	$K^{\text{KSA}}$	$K^{\text{RPA}}$
0	1.117	0.089	0.094	0.109
0.05	1.116	0.090	0.095	0.109
0.10	1.113	0.090	0.095	0.109
0.20	1.103	0.084	0.089	0.106
0.50	1.049	0.043	0.046	0.067
0.80	0.983	0.007	0.008	0.029
1.00	0.942	-0.009	-0.008	0.012
1.33	0.880	-0.024	-0.024	-0.007
1.60	0.837	-0.031	-0.031	-0.016
2.00	0.782	-0.036	-0.036	-0.024
2.29	0.748	-0.038	-0.038	-0.028
2.67	0.709	-0.038	-0.038	-0.030
3.20	0.663	-0.038	-0.038	-0.031
4.00	0.608	-0.036	-0.036	-0.031
5.33	0.540	-0.032	-0.032	-0.029
8.00	0.452	-0.026	-0.026	-0.024
10.00	0.408	-0.022	-0.022	-0.021
12.50	0.367	-0.019	-0.019	-0.018
16.67	0.320	-0.015	-0.015	-0.015
20.00	0.293	-0.013	-0.013	-0.013
25.00	0.262	-0.011	-0.011	-0.011

TABLE IV. Computed values of potential energy  $P$  and excess kinetic energy  $K$  per particle as a function of  $\tau = kT/\epsilon_F$  for  $r_s = 2.00$ . The excess kinetic energy is given for the convolution approximation (CA), the Kirkwood superposition approximation (KSA) and the random-phase approximation (RPA). All energies are in rydbergs.

$\tau$	$-P$	$K^{\text{CA}}$	$K^{\text{KSA}}$	$K^{\text{RPA}}$
0	0.602	0.059	0.063	0.080
0.05	0.601	0.059	0.063	0.080
0.10	0.600	0.060	0.063	0.081
0.20	0.597	0.058	0.062	0.080
0.50	0.580	0.046	0.049	0.070
0.80	0.557	0.031	0.033	0.054
1.00	0.541	0.023	0.024	0.044
1.33	0.515	0.013	0.013	0.032
1.60	0.496	0.007	0.008	0.024
2.00	0.471	0.002	0.002	0.016
2.29	0.455	-0.001	-0.001	0.011
2.67	0.436	-0.003	-0.003	0.007
3.20	0.412	-0.005	-0.005	0.003
4.00	0.383	-0.007	-0.007	-0.001
5.33	0.346	-0.008	-0.008	-0.004
8.00	0.296	-0.008	-0.008	-0.005
10.00	0.270	-0.007	-0.007	-0.006
12.50	0.245	-0.007	-0.007	-0.005
16.67	0.216	-0.006	-0.006	-0.005
20.00	0.198	-0.005	-0.005	-0.004
25.00	0.179	-0.004	-0.004	-0.004

TABLE V. Computed values of potential energy  $P$  and excess kinetic energy  $K$  per particle as a function of  $\tau = kT/\epsilon_F$  for  $r_s = 3.39$ . The excess kinetic energy is given for the convolution approximation (CA), the Kirkwood superposition approximation (KSA), and the random-phase approximation (RPA). All energies are in rydbergs.

$\tau$	$-P$	$K^{CA}$	$K^{KSA}$	$K^{RPA}$
0	0.376	0.041	0.044	0.062
0.05	0.376	0.041	0.044	0.062
0.10	0.376	0.041	0.044	0.062
0.20	0.374	0.041	0.043	0.062
0.50	0.368	0.036	0.039	0.059
0.80	0.358	0.030	0.031	0.052
1.00	0.351	0.025	0.026	0.047
1.33	0.339	0.019	0.020	0.038
1.60	0.329	0.015	0.016	0.033
2.00	0.316	0.011	0.011	0.026
2.29	0.307	0.009	0.009	0.022
2.67	0.297	0.006	0.006	0.018
3.20	0.283	0.004	0.004	0.014
4.00	0.267	0.002	0.002	0.009
5.33	0.244	0.000	0.000	0.005
8.00	0.212	-0.002	-0.002	0.001
10.00	0.195	-0.002	-0.002	0.000
12.50	0.179	-0.002	-0.002	-0.001
16.67	0.159	-0.002	-0.002	-0.001
20.00	0.147	-0.002	-0.002	-0.001
25.00	0.133	-0.002	-0.002	-0.001

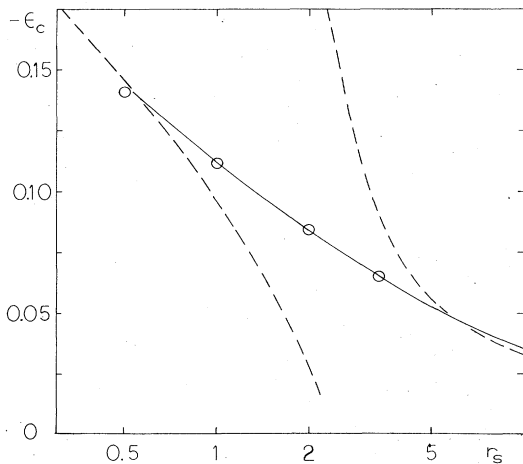


FIG. 1. Comparison of ground-state correlation energies (excess energy minus exchange energy) in rydbergs obtained here with those obtained in Ref. 13 by minimizing the energy. Solid line, correlation energies from Ref. 13 using convolution approximation; circles, correlation energies obtained here using convolution approximation in the energy but using methods of Sec. II to compute the Slater sum; dashed lines, high- and low-density expansion.

$$p = p - p_I, \quad (3.23)$$

is to use the virial theorem

$$p_v = \frac{1}{3}\rho(2K + P). \quad (3.24)$$

However, this method has a serious drawback when used in conjunction with a variational method. While a small error in the variational parameter causes only a small change in the total energy, it causes larger changes in the potential and kinetic energies, thereby greatly altering the pressure.

What is obviously needed is a method which takes advantage of the relative accuracy of the total energy. Such a method consists of integrating the energy over  $\beta$  at a constant density to obtain the excess Helmholtz free energy

$$\beta A(\beta) = \beta_0 A(\beta_0) + \int_{\beta_0}^{\beta} E(\beta') d\beta'. \quad (3.25)$$

The infinite-temperature limit of the excess free energy is zero because the interactions become negligible at sufficiently high temperatures and the energy and free energy of the system go over to those for an ideal gas. Once we have obtained  $A(\beta, \rho)$ , we can get the excess pressure by differentiating  $A$  with respect to volume, holding the temperature fixed

$$p_A = -N \left( \frac{\partial A}{\partial \Omega} \right)_T \quad (3.26)$$

or

$$p_A = \rho^2 \left( \frac{\partial A}{\partial \rho} \right)_T. \quad (3.27)$$

Once we have the excess free energy as a function of density and temperature, it is also possible to obtain the excess entropy per particle from

$$s = \beta(\epsilon - A) \quad (3.27)$$

and other thermodynamic quantities such as the specific heat.

#### IV. NUMERICAL METHODS AND RESULTS

The numerical methods used were generally those used in Refs. 13 and 20. If we let  $u_t = u_I + u$  denote the total quantum pair potential, we divide  $u_t$  into short- and long-range parts to solve the HNC integral equation.

$$u_t(r) = u_{sr}(r) + u_{lr}(r). \quad (4.1)$$

At high temperatures  $u_{sr}(r)$  is taken to be the ideal-Fermi-gas effective potential

$$u_{sr}(r) = u_I(r) = G_I(r) - \ln G_I(r) - C_I(r) \quad (\text{high } T) \quad (4.2)$$

TABLE VI. Negative of the excess free energy per particle in rydbergs as a function of  $\tau = kT/\epsilon_F$  and  $r_s$ , computing from Eq. (3.25) using the excess energy computed using the convolution approximation.

$\tau$	$r_s$			
	0.50	1.00	2.00	3.39
0	1.972	1.027	0.542	0.335
0.05	1.920	1.006	0.534	0.332
0.10	1.875	0.988	0.527	0.328
0.20	1.793	0.955	0.514	0.322
0.50	1.575	0.866	0.479	0.305
0.80	1.396	0.789	0.448	0.290
1.00	1.298	0.746	0.429	0.281
1.33	1.167	0.684	0.402	0.267
1.60	1.083	0.644	0.383	0.257
2.00	0.983	0.594	0.359	0.243
2.29	0.925	0.564	0.344	0.235
2.67	0.860	0.530	0.327	0.225
3.20	0.787	0.491	0.306	0.213
4.00	0.704	0.445	0.282	0.198
5.33	0.605	0.389	0.251	0.179
8.00	0.484	0.318	0.210	0.152
10.00	0.427	0.284	0.189	0.139
12.50	0.375	0.252	0.171	0.126
16.67	0.314	0.215	0.148	0.111
20.00	0.280	0.194	0.135	0.102
25.00	0.241	0.170	0.120	0.092

where  $C_I$  is the direct correlation function

$$\tilde{C}_I(K) = \rho^{-1} \{1 - [S_I(K)]^{-1}\}. \quad (4.3)$$

At low temperatures we used Stevens' method<sup>13</sup>

$$u_{sr}(r) = G_I(r) - \ln G_I(r), \quad (\text{low } T) \quad (4.4)$$

$$u_{Ir}(r) = u(r) - C_I(r). \quad (4.5)$$

All calculations were performed with 15-digit arithmetic using 512 points and the increment  $\Delta k = k_F/16$ . The numerical Fourier transforms were calculated using Filon's method.<sup>23</sup> Range-increment tests were carried out at the two extreme densities for five different temperatures.

The integrations to obtain the energy were done using the methods described in Ref. 13. The excess free energy was computed as a function of  $\tau$  and  $r_s$  by assuming that  $\epsilon$  was a linear function of  $\tau$  between the data points. This assumption was checked by assuming  $\epsilon$  to be a linear function of  $\beta$  between the data points; the maximum difference in the excess pressure was 0.5%. Above the highest temperature  $\epsilon$  was assumed to be given by the classical linearized Debye-Huckel (LDH) approximation.

$$\epsilon \cong -\left(\frac{9\pi}{4}\right)^{-1/3} \left(\frac{6}{\tau r_s}\right)^{1/2} \text{ Ry}, \quad \tau > 25 \quad (4.6)$$

In addition between  $\tau = 0$  and  $\tau = 0.05$ , the excess energy was assumed to increase from its ground-state value as  $T^2$ . The excess free energy ob-

tained from the CA for the energy is given in Table VI.

If we let

$$x = r_s^n \quad (4.7)$$

and change the variables in Eq. (3.27), we can write the pressure as

$$\frac{p_A}{\rho} = \frac{A(x, \tau)}{3} - \frac{nx}{3r_s} \left( \frac{\partial [r_s A(x, \tau)]}{\partial x} \right)_{\tau} - \left( \frac{2\tau}{3} \frac{\partial A(x, \tau)}{\partial \tau} \right)_x. \quad (4.8)$$

A quadratic polynomial in  $x$  was used to fit  $r_s A$  by a least-squares method at each  $\tau$  and the coefficients used to determine the derivative appearing in Eq. (4.8). Seventy per cent confidence limits were also estimated from the fit. The fit was done for both  $n = 0.5$  and  $n = -0.5$ , with  $n = 0.5$  found to be better. Figure 2 illustrates  $p_A^{CA}$  for four densities as a function of  $\tau$ . Table VII gives the  $p_A$  for the CA as a function of temperature and density.

Figures 3 and 4 compare  $p_A$  and  $p_v$  for both the RPA and the CA at two different densities. It is seen that while the two  $p_v$ 's differ considerably, the two  $p_A$ 's are in excellent agreement. This implies that the derivative of the energy is much more accurate than the potential energies and kinetic energies separately. Thus, reasonably accurate pressures may be obtained even if the RPA is used, provided one gets the pressure from the free energy, rather than from the virial expression for the pressure.

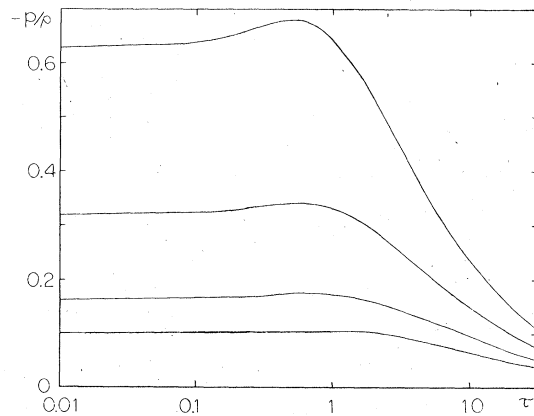


FIG. 2. Excess pressure divided by density in rydbergs as a function of  $\tau = kT/\epsilon_F$  for four densities. The pressures were computed by differentiating the excess free energy which was obtained from the excess energy computed using the convolution approximation for the three-body correlation function. The four densities are, from top to bottom,  $r_s = 0.5, 1.0, 2.0,$  and  $3.39$ .

TABLE VII. Values of  $-p^{CA}/\rho$ , the excess pressure divided by the density in rydbergs computed from the excess free energy using Eq. (4.8). Values given are for the convolution approximation. The Kirkwood superposition approximation and the random-phase approximation results differ by 0.006 at most.

$r_s$	0.50	1.00	2.00	3.39
$\tau$				
0	0.623	0.319	0.165	0.101
0.05	0.633	0.323	0.167	0.102
0.10	0.640	0.325	0.167	0.102
0.20	0.654	0.329	0.169	0.103
0.50	0.684	0.341	0.173	0.105
0.80	0.670	0.340	0.174	0.107
1.00	0.649	0.334	0.173	0.107
1.33	0.608	0.320	0.170	0.106
1.60	0.576	0.309	0.166	0.105
2.00	0.533	0.292	0.160	0.102
2.29	0.505	0.280	0.156	0.100
2.67	0.473	0.267	0.151	0.098
3.20	0.436	0.250	0.144	0.095
4.00	0.390	0.229	0.134	0.090
5.33	0.335	0.202	0.122	0.083
8.00	0.267	0.166	0.104	0.073
10.00	0.233	0.148	0.094	0.067
12.50	0.202	0.131	0.085	0.062
16.67	0.166	0.111	0.074	0.055
20.00	0.145	0.099	0.068	0.051
25.00	0.120	0.085	0.060	0.046

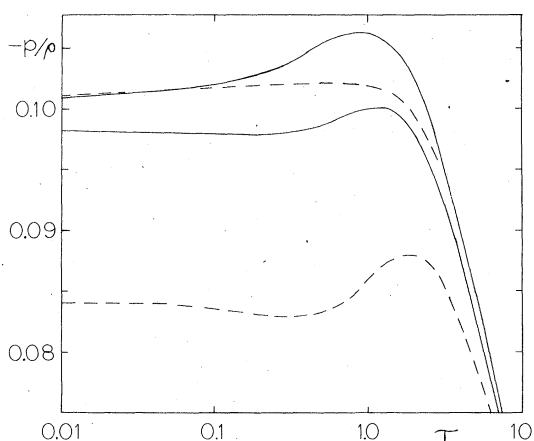


FIG. 3. Excess pressure divided by density in rydbergs as a function of  $\tau = kT/\epsilon_F$  for  $r_s = 3.39$ . The solid lines were computed using the convolution approximation for the three-body correlation function, the dashed lines used the random-phase approximation. In each case the upper curves were calculated from the excess free energy, Eq. (4.8), and the lower curves were calculated from the virial theorem, Eq. (3.24). It is seen that the excess pressures computed from the free energy agree much better than those computed from the virial theorem.

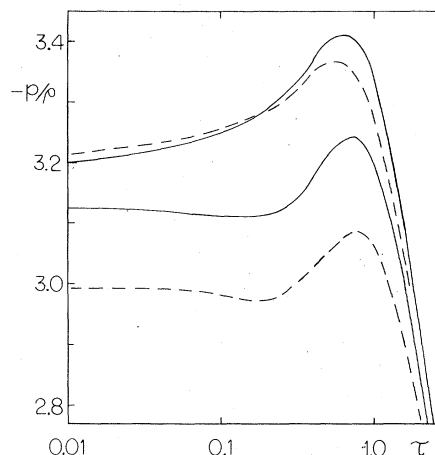


FIG. 4. Excess pressure divided by density in rydbergs as a function of  $\tau = kT/\epsilon_F$  for  $r_s = 0.5$ . The solid lines were computed using the convolution approximation for the three-body correlation function, the dashed lines used the random-phase approximation. In each case the upper curves were calculated from the excess free energy, Eq. (4.8), and the lower curves were calculated from the virial theorem, Eq. (3.24). It is seen that the excess pressures computed from the free energy agree much better than those computed from the virial theorem.

## V. DISCUSSION AND CONCLUSIONS

It is the author's belief that the CA does a better job of approximating the kinetic energy than does the KSA, which in turn is better than the RPA. This belief is based in large part on the fact that if one computes the ground-state energy from both Eq. (3.13) [which comes from Eq. (3.7)] and an alternative expression which comes from Eq. (3.7) before it is integrated by parts, the three-body approximation enters the two results in different manners and results in terms with approximately the same magnitude, but opposite signs. For  $r_s = 3.39$ , the two equations gave excess energies of  $-0.3334$  and  $-0.3347$  Ry in the CA. This difference was about one-fifth that in the KSA and about one-fifteenth that in the RPA. The agreement between the virial pressure and that obtained from the free energy is also much better when the CA is used for the three-body terms. Also, in Ref. 13, the CA was slightly preferred to the KSA because the minimum of the CA energy functional was in somewhat better agreement with the Dunn-Broyles functional.<sup>10</sup> For these reasons the author believes that the CA results are the most accurate of those studied; the RPA and KSA results, where included, are for comparison purposes only.

The classical  $\Gamma$  which gives the same asymptotic form of  $u$  ranges from 0 to 0.82 for  $r_s = 0.5$

and from 0 to 2.13 for  $r_s = 3.39$ . We expect that the HNC approximation has introduced negligible error since the HNC integral equation applied to the classical OCP is in excellent agreement<sup>20</sup> with Monte Carlo results for this range of  $\Gamma$ .

The ideal-Fermi-gas effective pair potential<sup>4,5</sup> is considered to be adequate for the electron gas. The ground-state calculation<sup>13</sup> and its agreement with the high-density expansion for the correlation energy tend to confirm this. At lower densities it becomes less important. There is a way of improving the ideal gas effective potential by including three-body and higher terms, but this would preclude the use of integral equations.<sup>24</sup>

Some of the effects of neglecting  $Y$  and  $Y_I$  are investigated in the Appendix. In the zero-density limit this approximation appears to cause only a very small error.<sup>7</sup>

The parametrized form chosen for  $u$ , Eq. (2.14), may be too restrictive. In particular, it may be this form which causes the magnitude of the excess pressure to first rise before finally dropping to zero as  $\tau$  increases. The obvious solution is to add one or more additional parameters and repeat the entire calculation. This requires no fundamental change, only more computer time.

By far the most serious source of error appears to be the approximations made in Sec. II in order to obtain the parameter in  $u$ . The low density-low temperature region is most seriously affected by these approximations. The RPA and GBSC structure factor can be replaced by the CA and HNC equation in the calculation of Sec. II. This should greatly improve the accuracy and enable the calculation to be extended to  $r_s > 3.39$ . The results shown in Fig. 1 indicate that even with the approximations of Sec. II we were able to obtain excellent agreement with Stevens<sup>13</sup> correlation energies at  $T=0$ .

#### ACKNOWLEDGMENTS

The author is indebted to Dr. R. L. Coldwell and Professor A. A. Broyles for helpful discussions and for critical comments on the manuscript.

#### APPENDIX: ALTERNATIVE METHODS FOR OBTAINING ENERGIES AND PRESSURES

This appendix presents two methods for obtaining the energy and pressure which gave poor results compared to those obtained in the main text of this paper. These methods are included here because they may be more accurate for systems other than the OCP. In addition, they give us some information about the size of  $Y$  and  $Y_I$ .

The first method starts from the differential equation for the total quantum potential,  $U_t = U$

+  $U_I$ , Eq. (2.3). We substitute this equation into Eq. (3.3) and integrate by parts to obtain

$$E = \frac{3N}{2\beta} + \frac{1}{Z} \int e^{-U_t} \left( V_{ct} + \frac{\hbar^2}{8m} \sum_i \nabla_i U_t \cdot \nabla_i U_t + Y \right) dR. \quad (A1)$$

We subtract the corresponding equation for the ideal gas and reduce the integrals to get

$$\epsilon = P + K, \quad (A2)$$

where

$$K = \frac{\hbar^2 \rho^2}{8m} \int \{ \nabla G \cdot \nabla u + \nabla(G - G_I) \cdot \nabla u_I \} d\vec{r} + \frac{1}{N} (\langle Y \rangle - \langle Y_I \rangle), \quad (A3)$$

where the  $\langle Y \rangle$  denotes the expectation value taken over the ensemble. The last term involving  $Y$  and  $Y_I$  cannot be determined and must be neglected. The energy from Eq. (A3) is illustrated in Figs. 5 and 6 for two densities and is compared with the energy obtained for the CA.

The second method is an attempt to calculate the pressure by analytically performing the cancellations in the virial expression for the pressure. Using Eqs. (2.3) and (3.3) in the virial expression for the total pressure, we get

$$p_t \Omega = \frac{N}{\beta} + \frac{1}{3Z} \int e^{-U_t} \left( 2Y - \sum_i \vec{r}_i \cdot \nabla_i V_{ct} + \frac{\hbar^2}{2m} \sum_i (\nabla_i^2 U_t - \frac{1}{2} \nabla_i U_t \cdot \nabla_i U_t) \right) dR, \quad (A4)$$

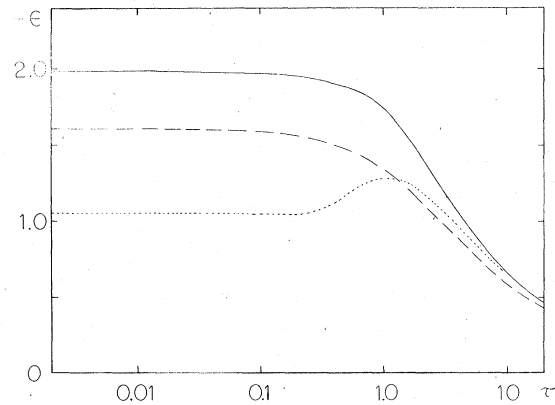


FIG. 5. Comparison of excess energies in rydbergs obtained by three methods as a function of  $\tau = kT/\epsilon_F$  for  $r_s = 0.50$ . Solid line, convolution approximation for three-body correlation function, Eq. (3.18); dashed line, Eq. (A3); dotted line, Eq. (A11).

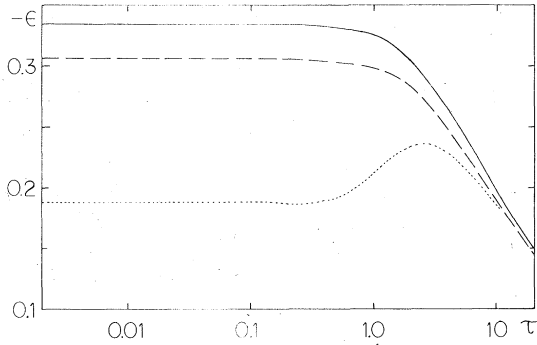


FIG. 6. Comparison of excess energies in rydbergs obtained in three methods as a function of  $\tau = kT/\epsilon_F$  for  $r_s = 3.39$ . Solid line, convolution approximation for three-body correlation function, Eq. (3.18); dashed line, Eq. (A3); dotted line, Eq. (A11).

where we have also used

$$V_{cl} = - \sum_j \vec{r}_j \cdot \nabla_j V_{cl}. \quad (\text{A5})$$

If we solve Eq. (2.3) for  $V_{cl}$  and substitute it into Eq. (A4) we get

$$p_t \Omega = \frac{N}{\beta} + \frac{1}{3Z} \int e^{-U_t} \left[ 2Y + \sum_j \vec{r}_j \cdot \nabla_j \times \left( Y - \frac{\partial U}{\partial \beta} \right) \right] dR + I_s, \quad (\text{A6})$$

where  $I_s$  represents those terms which may be combined to give a sum of surface integrals:

$$I_s = \frac{\hbar^2}{12mZ} \sum_l \sum_j \int \nabla_l \cdot [e^{-U_t} \nabla_l (\vec{r}_j \cdot \nabla_j U_t)] dR. \quad (\text{A7})$$

If we subtract the corresponding expression for an ideal gas and assume that the surface integrals vanish, then we have

$$p = - \frac{\rho^2}{6} \int \left( G\vec{r} \cdot \nabla \frac{\partial u}{\partial \beta} + (G - G_I)\vec{r} \cdot \nabla \frac{\partial u_I}{\partial \beta} \right) d\vec{r} + \frac{1}{3\Omega} I_Y, \quad (\text{A8})$$

where

$$I_Y = \left\langle 2Y + \sum_j \vec{r}_j \cdot \nabla_j Y \right\rangle - \left\langle 2Y_I + \sum_j \vec{r}_j \cdot \nabla_j Y_I \right\rangle. \quad (\text{A9})$$

This expression may then be used to obtain a formula for the excess energy by using the virial theorem to give

$$\epsilon = \frac{1}{2} P + \frac{3}{2} p / \rho \quad (\text{A10})$$

or

$$\epsilon = \frac{P}{2} - \frac{\rho}{4} \int \left( G\vec{r} \cdot \nabla \frac{\partial u}{\partial \beta} + (G - G_I)\vec{r} \cdot \nabla \frac{\partial u_I}{\partial \beta} \right) d\vec{r} + \frac{1}{2N} I_Y. \quad (\text{A11})$$

The resulting energies, neglecting  $I_Y$  are plotted in Figs. 5 and 6.

We neglected  $Y - Y_I$  in determining the energy in Sec. III. However, the excellent agreement with the high-density expansion for the energy at  $r_s = 0.5$  indicates that the expectation value of  $Y - Y_I$  is very small, or

$$\langle Y \rangle \approx \langle Y_I \rangle. \quad (\text{A12})$$

Comparing the results from Eq. (A3) with the CA excess energy obtained from Eq. (3.18) then gives us an estimate of  $\langle Y_I \rangle - \langle Y_I \rangle_I$ . The difference between the excess energies obtained from Eq. (A3) and Eq. (A11) then allow us to estimate the size of the term

$$\left\langle \sum_j \vec{r}_j \cdot \nabla_j Y \right\rangle - \left\langle \sum_j \vec{r}_j \cdot \nabla_j Y_I \right\rangle. \quad (\text{A13})$$

From Figs. 5 and 6, we see that  $\langle Y_I \rangle - \langle Y_I \rangle_I$  is fairly small for large  $r_s$  but becomes large relative to the excess energy as  $r_s$  becomes small, presumably because  $Y_I$  becomes large.

\*Work supported in part by a grant from the NSF.

†Present address: 5447 Harden Ave., Orange Park, Florida 32073.

<sup>1</sup>R. P. Beres and M. A. Pokrant, J. Chem. Phys. **64**, 5095 (1976).

<sup>2</sup>M. A. Pokrant, A. A. Broyles, and R. L. Coldwell, Int. J. Quantum Chem. **8S**, 403 (1974).

<sup>3</sup>R. L. Coldwell, M. A. Pokrant, and A. A. Broyles, in *Quantum Statistics and the Many-Body Problem*, edited by S. B. Trickey, W. P. Kirk, and J. W. Dufty (Plenum, New York, 1975), pp. 271-277.

<sup>4</sup>F. Lado, J. Chem. Phys. **47**, 5369 (1967).

<sup>5</sup>F. A. Stevens, Jr. and M. A. Pokrant, J. Chem. Phys. **61**, 3768 (1974); **62**, 4588 (E) (1975).

<sup>6</sup>J. M. van Leeuwen, J. Groeneveld, and J. de Boer, Physica (The Hague) **25**, 792 (1959); E. Meeron, J. Math. Phys. **1**, 192 (1960); Prog. Theor. Phys. **24**, 588 (1960); T. Morita, *ibid.* **20**, 920 (1958); **21**, 361 (1959); **23**, 175 (1960); **23**, 829 (1960); T. Morita and K. Hiroike, *ibid.* **23**, 385 (1960); **23**, 1003 (1960); M. S. Green, Hughes Aircraft Company Report, 1959 (unpublished); L. Verlet, Nuovo Cimento **18**, 77 (1960); G. S. Rushbrooke, Physica (The Hague) **26**, 259 (1960).

<sup>7</sup>M. A. Pokrant, A. A. Broyles, and Tucson Dunn, Phys. Rev. A **10**, 379 (1974).

<sup>8</sup>H. J. Shin, doctoral dissertation (University of Florida, 1973) (unpublished).

<sup>9</sup>D. Bohm and D. Pines, Phys. Rev. **92**, 609 (1953).

- <sup>10</sup>T. Dunn and A. A. Broyles, *Phys. Rev.* **157**, 156 (1967).
- <sup>11</sup>A. A. Broyles and T. Dunn, *Int. J. Quantum Chem.* **1S**, 803 (1967).
- <sup>12</sup>T. Gaskell, *Proc. Phys. Soc. Lond.* **77**, 1182 (1961); A. A. Broyles and H. L. Sahlin, *Bull. Amer. Phys. Soc.* **8**, 32 (1963); A. A. Broyles, H. L. Sahlin, and D. D. Carley, *Phys. Rev. Lett.* **10**, 319 (1963).
- <sup>13</sup>F. A. Stevens, Jr. and M. A. Pokrant, *Phys. Rev. A* **8**, 990 (1973).
- <sup>14</sup>M. S. Becker, A. A. Broyles, and T. Dunn, *Phys. Rev.* **175**, 224 (1968).
- <sup>15</sup>R. Monnier, *Phys. Rev. A* **6**, 393 (1972).
- <sup>16</sup>M. A. Pokrant and F. A. Stevens, Jr., *Phys. Rev. A* **7**, 1630 (1973); *A* **8**, 2202(E) (1973).
- <sup>17</sup>See, for example, P. Henrici, *Discrete Variable Methods in Ordinary Differential Equations* (Wiley, New York, 1962), p. 67.
- <sup>18</sup>J. G. Kirkwood, *J. Chem. Phys.* **3**, 300 (1935).
- <sup>19</sup>H. W. Jackson and E. Feenberg, *Rev. Mod. Phys.* **34**, 686 (1962).
- <sup>20</sup>J. F. Springer, M. A. Pokrant, and F. A. Stevens, Jr., *J. Chem. Phys.* **58**, 4863 (1973); K. C. Ng, *ibid.* **61**, 2680 (1974).
- <sup>21</sup>M. Gell-Mann and K. A. Brueckner, *Phys. Rev.* **106**, 364 (1957); W. J. Carr, Jr. and A. A. Maradudin, *ibid.* **133**, A371 (1964).
- <sup>22</sup>W. J. Carr, Jr., R. A. Coldwell-Horsefall, and A. E. Fein, *Phys. Rev.* **124**, 747 (1961).
- <sup>23</sup>See, for example, C. J. Tranter, *Integral Transforms in Mathematical Physics* (Wiley, New York, 1966), p. 67.
- <sup>24</sup>M. A. Pokrant, *J. Chem. Phys.* **62**, 4959 (1975).